© 1994 Wiley-Liss, Inc.

Cytometry 16:236–242 (1994)

Lissajous-Like Patterns in Scatter Plots of Calibration Beads

R.M.P. Doornbos, A.G. Hoekstra, K.E.I. Deurloo, B.G. De Grooth[1], P.M.A. Sloot, and J. Greve

Applied Optics Group, Faculty of Applied Physics, University of Twente, Enschede (R.M.P.D., K.E.I.D., B.G.D.G., J.G.), and Parallel Scientific Computing and Simulation Group, Department of Computer Systems, Faculty of Mathematics and Computer Science, University of Amsterdam, Amsterdam (A.G.H., P.M.A.S.), The Netherlands

Received for publication October 12, 1993; accepted February 21, 1994

Flow cytometric measurements of light scattering of polystyrene calibration beads revealed remarkable Lissajous-like loops in two-parameter scatter plots. The existence of such loops is shown to be in qualitative agreement with Lorenz-Mie scattering theory of homogeneous spheres. The occurrence of these patterns reflects the extreme particle size dependency of perpendicular light scattering of homogeneous spheres. These effects may give an explanation for the frequently observed phenomenon that polystyrene spheres reveal a relatively large CV in the perpendicular light scattering signals, whereas the CV of the forward light scattering signal is small. We conclude that one should be careful to optimize the perpendicular light scattering channel by minimizing the CV, because there is no linear relationship between instrument alignment quality and the CV of the perpendicular light scattering signals of calibration beads.

© 1994 Wiley-Liss, Inc.

Key terms: Polarization, alignment, calibration, instrumentation, flow cytometer, Lorenz-Mie theory, Mueller matrix, small particle light scattering

In flow cytometry scattered light is frequently used to obtain size or structural information from small particles. The amount and polarization of scattered light is a measure of the characteristics of the particle. For instance the signal from the forward scattering channel, which measures the intensities of mainly the first lobe in the angular intensity distribution, is strongly related to wavelength, refractive indices, and size of the particle (13,15). The granularity of cells strongly influences perpendicular scattered light (14). Also other characteristics of cells can influence the intensity of the scattered light, such as membrane ruffling (10) and nucleus area (3).

Explicit use of the polarization dependency of light scattering enables discrimination of eosinophils from neutrophilic granulocytes (5). This allows differentiation of human leukocytes into four major sub-populations without any preparation step other than lysing (17). To explain this phenomenon we are investigating the polarized scattering characteristics of leukocytes and trying to determine if other sub-populations can be separated.

In using calibration beads and non-conventional light polarizations we have encountered an at first sight strange phenomenon of Lissajous-like patterns in two-parameter scatter plots. In a previous article (8) we presented an explanation of these loops. We used the scattering theory of Lorenz and Mie and obtained a reasonable agreement with the measurements. In this article we stress the implications for flow cytometry. The presented results can be important for calibration and alignment procedures of flow cytometers which usually include measurements of light scattering of calibration beads.

MATERIALS AND METHODS

We have modified our flow cytometer (Fig. 1) to obtain a flexible system in which the polarization of the incident (P1) and the two scattered light paths (A1, A2) can be set and selected, respectively, by inserting either a quarter wave plate, a linear polarizer, or both. The setup has a 5 mW He-Ne laser (model 105–1, Spec-

[1]Address reprint requests to Dr. B.G. DeGrooth, Applied Optics Group, Faculty of Applied Physics, University of Twente, P.O. Box 217, 7500 AE Enschede, The Netherlands.

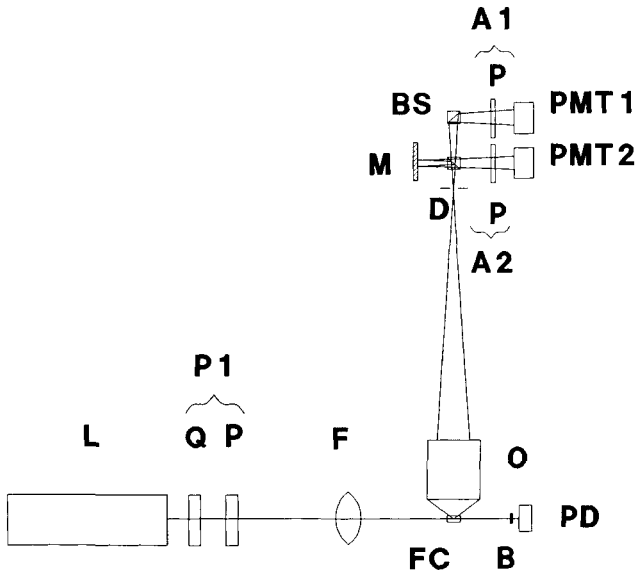

FIG. 1. Setup of a flow cytometer for polarization measurements. At positions P1, A1, and A2 a combination of quarter wave retarders and/or polarizers can be inserted. L: laser; Q: quarter wave retarder; P: linear polarizer; F: focusing lens; FC: flow cell; B: beam dump; PD: photodiode; O: microscope objective; D: diaphragm; M: mirror; BS: beamsplitters; PMT: photomultiplier.

tra Physics, Mountain View, CA) as light source and a 100 mm spherical lens to focus the light to a spherical spot (a diameter of 80 μm) in the flow cell. Forward scattered light (FLS, 2–6°) is detected with a PIN photodiode (PIN 10D, United Detector Technology, Santa Monica, CA); the perpendicular scattered light (PLS), collected by a 0.4 NA objective (20/0.4, Spindler Hoyer, Göttingen, Germany), is divided by beamsplitters and is detected with two head-on photomultipliers (R1104, Hamamatsu, Hamamatsu City, Japan). This setup with two beamsplitters and a mirror is chosen to enable compensation of the polarizing effect of the beamsplitters. In this way the light in the perpendicular direction is now travelling through the same components for both detectors, yielding a simplified calculation.

Our routine flow cytometer system consists of an Argon-ion laser (488 nm, max. 3 W, model 2020, Spectra Physics) focused to an elliptical spot (20*150 μm), a 0.6 NA objective (H32/0.60, Leitz, Wetzlar, Germany), and head-on photomultipliers (R1104, Hamamatsu). Forward scattered light (2–6°) is detected with a PIN photodiode (PIN 10D). Both flow cytometers use peak detection systems and signals are digitized with a 12 bits A/D converter (1).

The experiments were performed with polystyrene beads of different sizes: 7.040 ± 0.051 μm (Duke Scientific Corporation, Palo Alto, CA), and Fluoresbrite plain YG 2.23 ± 0.02 μm (Polysciences, Warrington, PA). The refractive indices of the beads and water used in our calculations was 1.5874 and 1.3318, respectively, at 632.8 nm, and 1.6033 and 1.3371, respectively, at 488.0 nm (7).

Alignment of the routine flow cytometer is performed with fluorescent beads. The alignment of the modified flow cytometer using only light scattering is not trivial as we try to point out in this article. We therefore use a procedure in which we first align the instrument on optimal FLS signals with small beads (1 μm). Second, we image the walls of the cuvette sharply on the diaphragm, carefully avoiding the light going through the opening. Running the beads we image the beads exactly on the diaphragm opening. This procedure is checked with fluorescent beads yielding always CVs below 3%.

We use the Mueller matrix formalism (4,12) in which scattering properties of a particle are described with intensities incident on and scattered from the object. The polarization of light is fully characterized by a (Stokes-) vector with four elements each giving the extent of one particular type of polarized light. The first element gives the total intensity (I), parameters Q, U, and V represent the extent of horizontal linear, 45° linear, and circular polarization, respectively. The 4 by 4 Mueller matrix describes the transition from incident to scattered light by the scattering object in one specific direction.

$$\begin{pmatrix} I_s \\ Q_s \\ U_s \\ V_s \end{pmatrix} = \frac{1}{k^2 r^2} \begin{bmatrix} S_{11} & S_{12} & S_{13} & S_{14} \\ S_{21} & S_{22} & S_{23} & S_{24} \\ S_{31} & S_{32} & S_{33} & S_{34} \\ S_{41} & S_{42} & S_{43} & S_{44} \end{bmatrix} \begin{pmatrix} I_i \\ Q_i \\ U_i \\ V_i \end{pmatrix}$$

The subscripts i and s stand for incident and scattered, respectively, k is the wave vector and r is the distance between object and detector.

A flow cytometer measures signals proportional to combinations of matrix elements integrated over the detection angles. If we consider a conventional setup with vertical polarized incident light (vector (1,−1, 0,0)·I_i), then a perpendicular light scattering (PLS) detector without analyzer (element I_s) measures an intensity proportional to (S11−S12)·I_i. These intensities result from integration over a solid angle with a half angle of, for instance, approximately 17.5° when using a 0.4 NA objective. The circular forward scattering (FLS) detector measures an intensity proportional to (S11−S12)·I_i integrated from 2° to 6° in our setup. Other combinations of matrix elements can be measured by changing the setup with regard to incident polarization and detected polarization, using optical elements such as polarizers and quarter wave plates (4,16).

The scattering of polystyrene calibration beads can be approximated by the scattering theory for homogeneous spheres, developed by Lorenz and by Mie (4,9,11,18). With this theory the internal and external fields of the sphere can be calculated analytically. The resulting non-zero matrix elements for an isotropic homogeneous sphere are S11, S22 (=S11), S12, S21 (=S12), S33, S44 (=S33), S34 and S43 (=−S34). Several computer programs exist to calculate the very complex S_{ij} functions in practical situations (2,4). We

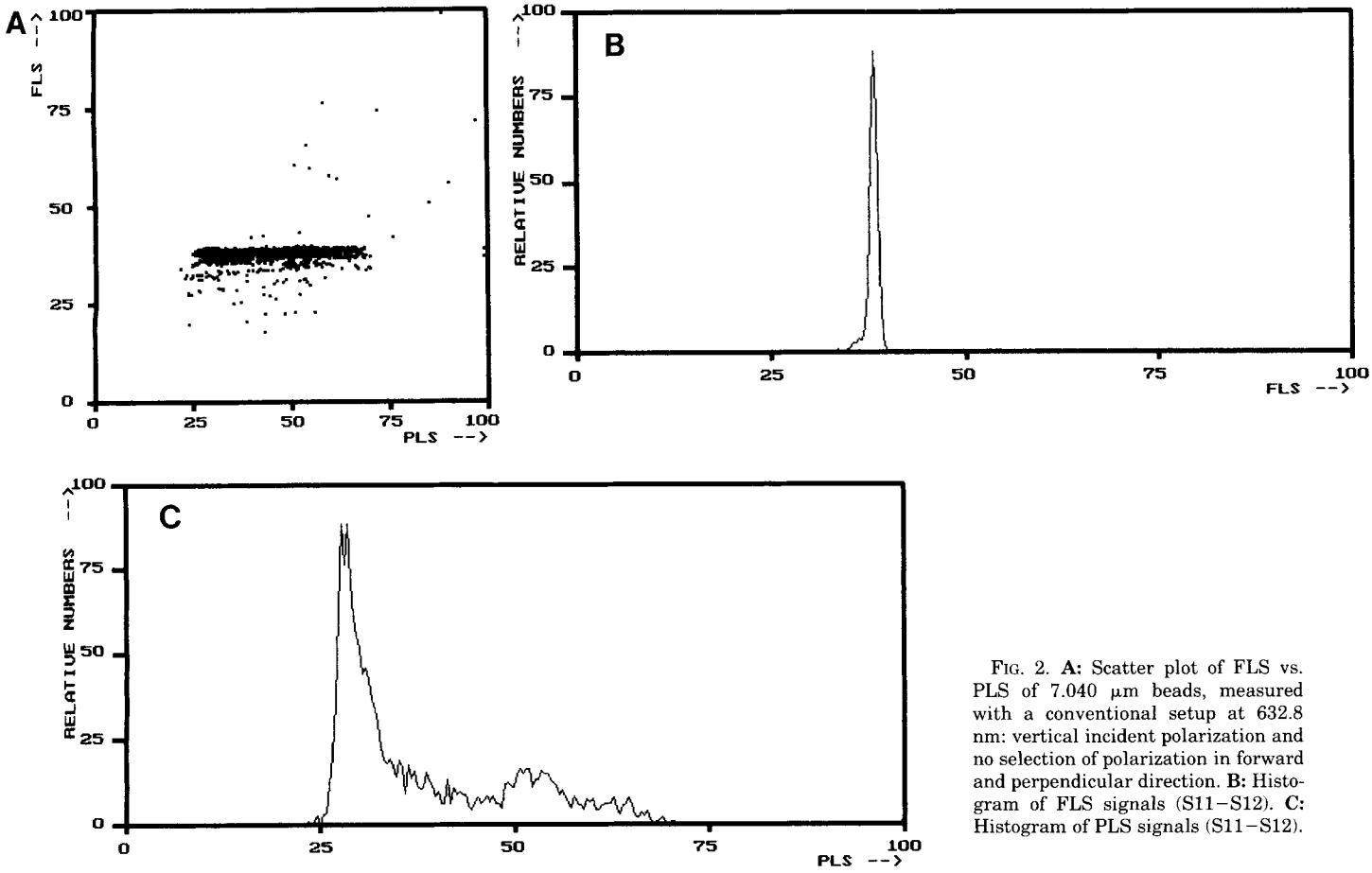

FIG. 2. **A:** Scatter plot of FLS vs. PLS of 7.040 μm beads, measured with a conventional setup at 632.8 nm: vertical incident polarization and no selection of polarization in forward and perpendicular direction. **B:** Histogram of FLS signals (S11−S12). **C:** Histogram of PLS signals (S11−S12).

have used the Bohren and Huffmann program (4), modified with an implementation of the generalized Lorenz-Mie theory; thus the Gaussian beam shape is taken into account (6). Comparison of theoretical calculations of the integrated matrix elements with measured data is performed as described elsewhere (8,16).

RESULTS

We have measured 7.040 μm beads using a conventional setup. The forward light scattering vs. perpendicular light scattering (FLS-PLS) plot is shown in Figure 2A. Clearly visible is the narrow distribution in the FLS signals (Fig. 2B). The PLS distribution is much broader, almost a bimodal distribution (Fig. 2C).

Figure 3A shows the scatter plot of two different matrix element combinations, S11+S12 vs. S11−S12, measured with our setup using an incident polarization at +45° and the detected polarization vertical and horizontal, respectively, in the two perpendicular detection channels. A triangular shape appears in the plot.

With different optical elements in position P1, A1, and A2 in the setup (Fig. 1) we have measured other matrix element combinations when the incident polarization is right circular and the detected polarization is +45 and −45°, and we obtain Figure 3B. An "eight"-like pattern appears in the scatter plot of the two parameters.

In an attempt to understand the cause of these phenomena we used the Lorenz-Mie theory to calculate the scattering of the beads. In Figure 4 the calculated angular dependence of the S11 element of a 7.040 μm polystyrene calibration bead is plotted. The two parts between the pairs of dashed lines in the figure are the ranges which are detected by the forward and perpendicular detectors. Other matrix elements (S12, S33, and S34) show similar patterns; however, the positions of the maxima and minima are slightly shifted in angle and height.

When the size of the bead increases, the calculated angular pattern (Fig. 4) shifts to smaller angles (4), so the maxima become more narrowly spaced. This results in a change of the detected signal, because a measured signal is proportional to a linear combination of matrix elements. This size dependence is not linear (note the log scale) and not monotonic, but more or less sinusoidal, as shown for two matrix element combinations in Figure 5A,B (this figure corresponds to the measurements of Fig. 3A,B). It is clear that different matrix element combinations show similar sinusoidal size dependencies, but the phase (that is, the maxima

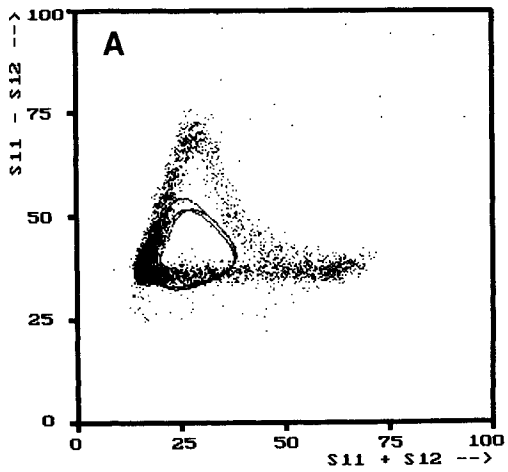

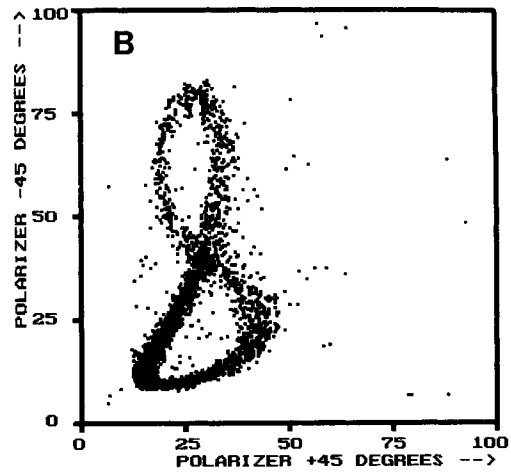

FIG. 3. **A:** Scatter plot of S11−S12 vs. S11 + S12 signals from 7.040 μm beads measured with the setup using an incident polarization at +45° and a vertical and horizontal, respectively, perpendicular detected polarization at 632.8 nm. The smooth line was calculated assuming a Gaussian size distribution (bead size range: 6.84 μm to 7.24 μm, wavelength is 632.8 nm). **B:** Scatter plot of 7.040 μm beads when the incident polarization is right circular and the perpendicular detected polarization is −45° and +45° (wavelength is 632.8 nm). This corresponds to S11 −0.62 · S33 −0.78 · S34 vs. S11 +0.62 · S33 +0.78 · S34.

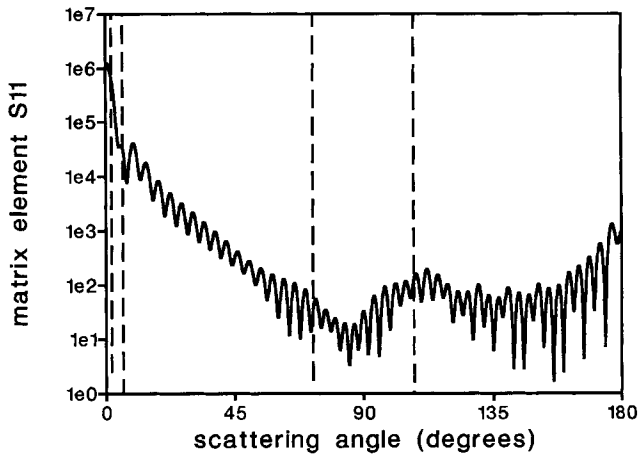

FIG. 4. Calculated angular dependency of the scattering matrix element S11 for a 7.040 μm bead with a refractive index of 1.5874 in water (refractive index 1.3318) and a wavelength of 632.8 nm. The regions between the pairs of dashed lines are the ranges detected by the forward (left side) and perpendicular detectors (middle).

occur at different bead diameters) and the exact shape (higher frequency components) are different. Therefore even for a narrow size distribution, a two-parameter plot should reveal Lissajous-like loops. When rotating in one direction along the loop (Fig. 3A,B) the size of the beads increases monotonically. With certain combinations of matrix elements the size dependence can be extremely strong: a change of 1% in diameter can result in a 700% change in signal (see Fig. 3B).

Using the specified CV of the beads and assuming a Gaussian size distribution, we have calculated the expected form of the scatter plot (8). An example is shown in Figure 3A, where the calculation results are mapped on measured data. The qualitative agreement of the measured "triangle" with the theoretical curve is remarkable and strongly supports our suggestion that the effects result from Lorenz-Mie type scattering.

Our hypothesis that the effects are probably caused by the extreme size dependence is described in detail elsewhere (8). Now we have tested this hypothesis further by using the forward light scattering signal as a measure of particle size. If we construct the histogram of the FLS signals from the two regions indicated in Figure 6A we obtain Figure 6B. Clearly the positions of the histograms are shifted, in agreement with theoretical expectations.

These results prompted us to question if similar effects could be observed using a conventional flow cytometer. In addition we investigated whether small size calibration beads would also show these effects. With our routine flow cytometer we have measured 2.23 μm fluorescent beads for which the FLS-PLS plot is shown in Figure 7. It should be noted that in the plot about 16,000 beads are displayed of which 93% are in the cluster at position FLS = 12 and PLS = 23. Both questions are answered directly: the perpendicular light scattering oscillates as a function of bead size. Since beads with different sizes gave similar scatter plots, the effect is not caused by one peculiar bead sample. We conclude that with all standard flow cytometers it should be possible to observe the described effects.

In Figure 7 an interesting phenomenon can be observed, that probably reflects the production process of the calibration beads. Beads are in general produced in a stepwise polymerization process. When during the early stages of this process two very small pre-beads

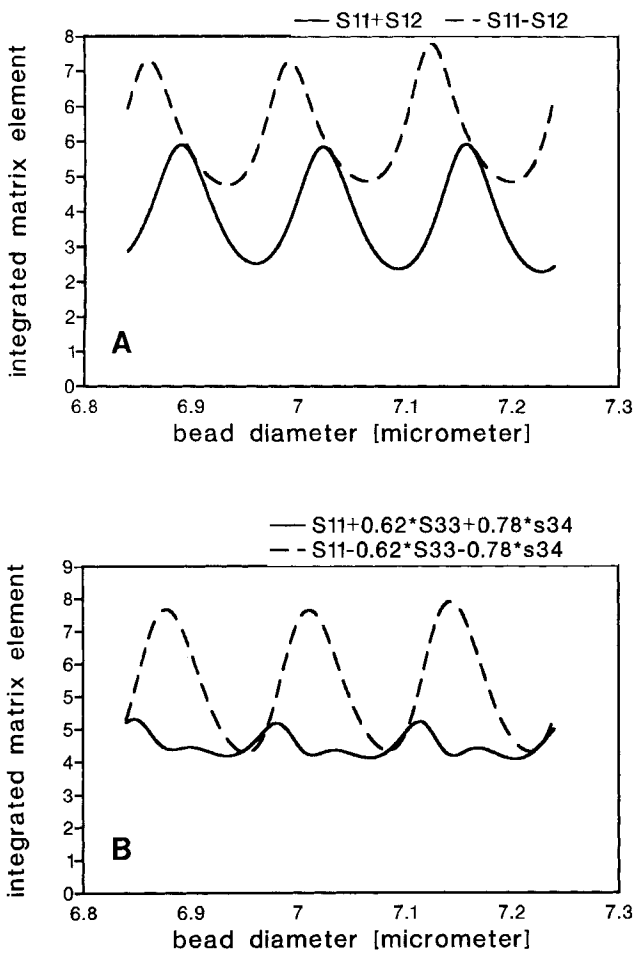

FIG. 5. **A:** Integrated matrix element combinations S11 + S12 and S11 − S12 (in perpendicular direction with angles determined by the numerical aperture of the objective: NA = 0.4) as a function of the bead size at 632.8 nm (same refractive indices as used for Fig. 4). **B:** Integrated matrix element combinations S11 + 0.62 · S33 + 0.78 · S34 and S11 − 0.62 · S33 − 0.78 · S34 (in perpendicular direction with angles determined by the numerical aperture of the objective: NA = 0.4) as a function of the bead size at 632.8 nm (same refractive indices as used for Fig. 4).

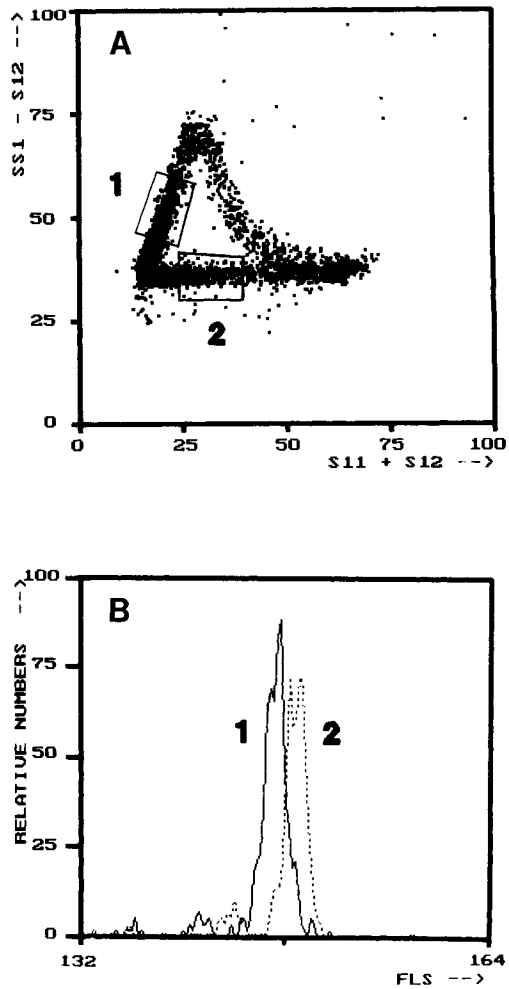

FIG. 6. **A:** Scatter plots of 7.040 μm beads at 632.8 nm: +45° vs. −45° plot (same experiment as in Fig. 3A). (**B**) gives the histograms of forward scattering signals of the particles inside gate 1 (solid line) and gate 2 (dotted line) in (A). Note the offset of the forward scattering axis.

are stuck together, the resulting bead will be slightly larger than a bead which started with a single pre-bead (D. Parks, private communications). This phenomenon can be seen in the scatter plot as small sub-clusters at different positions (indicated by the arrows). Measurements of the fluorescence indicate that the beads in regions 1 and 2 are not doublets or triplets.

We have calculated the forward and perpendicular light scattering signals of our routine flow cytometer setup for beads increasing in size from 0.1 to 10 μm diameter (with steps of 16 nm). In Figure 8A the forward scattering signal is plotted as a function of bead diameter. With increasing size the forward scattering signal oscillates slowly. The amplitude of the oscillation increases strongly above 2 μm and has its maximum around 4 μm. It is remarkable that beads with sizes around 3 μm have twice as high forward scattering signal as 4 μm beads. In Figure 8B the perpendicular light scattering signal is plotted as a function of the bead diameter. In contrast to forward scattering the perpendicular light scattering signal oscillates rather quickly. The amplitude of the oscillation increases between 2 and 4 μm and for diameters above 4 μm it remains roughly the same. Combining the curves of Figure 8A and B yields the theoretical prediction of the FLS-PLS scatter plot of beads (Fig. 8C). The signals of a sphere with increasing size follow the curve in Figure 8C: its FLS increases to a maximum value of about 90 units at size 1.6 μm, decreases again to 50 at size 2.1 μm, increases again to 490 at size 3.2 μm. Above a diameter of 2 μm the PLS starts to oscillate noticeably. Due to the decrease of FLS above 3.2 μm and the oscillating PLS the curve crosses itself. At a size of 4.0 μm the value of FLS has a local minimum

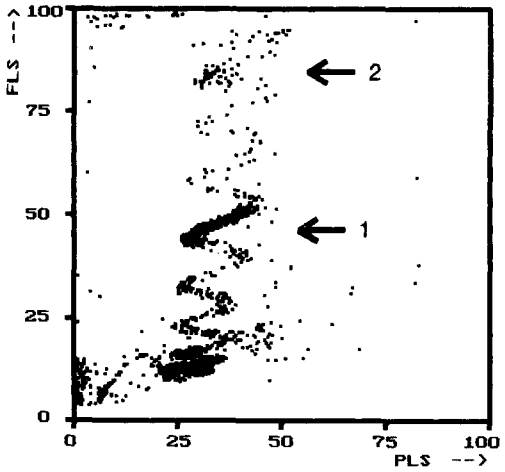

FIG. 7. Scatter plot of FLS vs. PLS of (about 16,000) 2.23 μm beads in a conventional routine flow cytometer using 488.0 nm light (integrated matrix elements S11 + S12 in forward direction vs. S11−S12 in perpendicular direction). Arrows 1 and 2 indicate probable sub-clusters of beads with larger diameter.

again at a value of about 210 and PLS oscillates between 6 and 10. Beads larger than 4 μm have again a higher FLS signal. It is surprising that overlap occurs for beads of different sizes.

The essential features observed in Figure 8C are also present in Figure 7. The region of Figure 8C that corresponds to the measurement of Figure 7 is roughly from beads with sizes from 1 to 3 μm (see insert, Fig. 8C). Note that even the smooth line of particles smaller than 2 μm is clearly visible. The measurements are done with absorbing spheres which means that the refractive index has a complex value. Therefore Figure 8C should not quantitatively be compared to Figure 7.

DISCUSSION

In this article we have shown that Lissajous-like patterns do occur in two-parameter dot plots when polystyrene beads are measured in a flow cytometer. The experiments support the hypothesis that the effects can largely be described by the Lorenz-Mie theory. The Lissajous-like patterns originate from the lobe structure of the matrix elements as a function of scattering angle (Fig. 4). This lobe structure changes with increasing size of the scattering sphere. The matrix elements, integrated over the detection angles, yield a sinusoidal dependence on the size (Fig. 5A). A measured signal is proportional to a linear combination of matrix elements; thus two-parameter dot plots will show Lissajous-like patterns. In general we have obtained a qualitative agreement between theory and experiments (see Figs. 3 and 7), but an accurate quantitative agreement could not be obtained yet (8).

The "eight"-like pattern of Figure 3B still puzzles us, because the calculated pattern cannot be matched to the measured pattern. The double and higher "frequen-

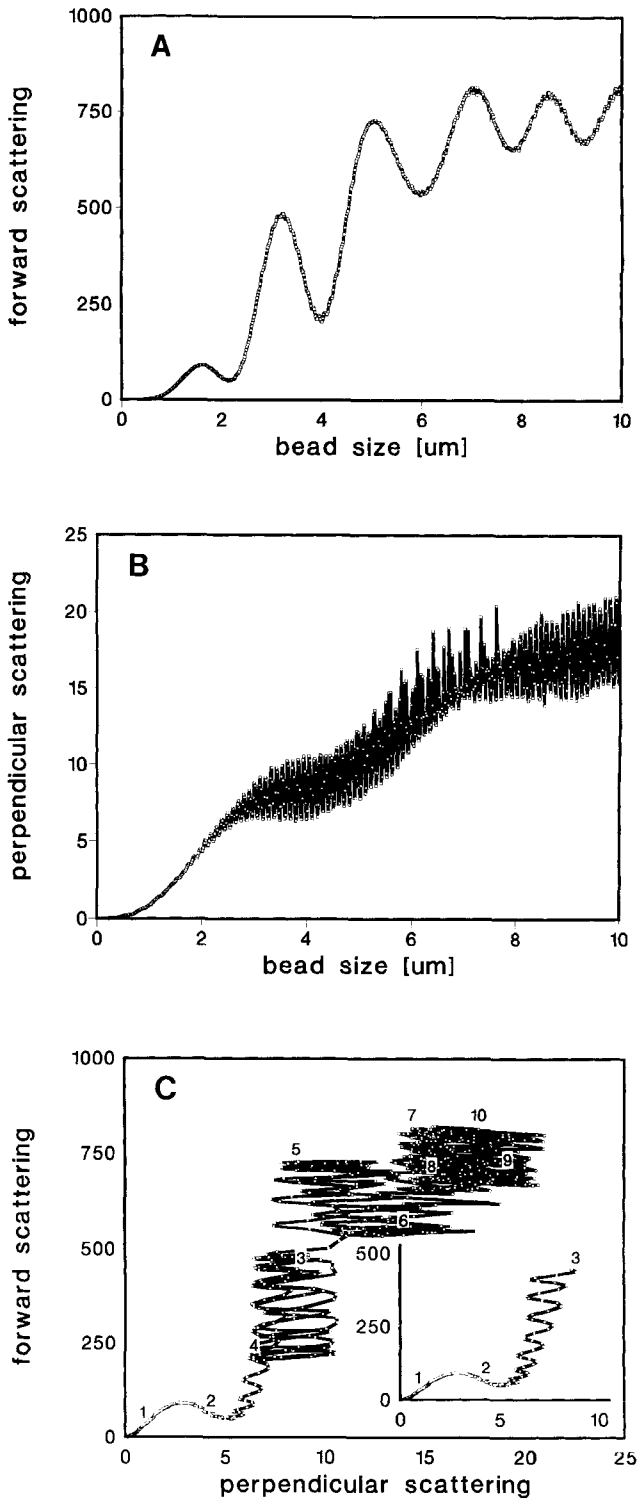

FIG. 8. **A:** Calculated forward scattering signals as a function of bead size from 0.1 to 10 μm diameter (with steps of 16 nm) for our routine flow cytometer at 488.0 nm. **B:** Calculated perpendicular light scattering signals as a function of bead size. **C:** A theoretical prediction of the FLS-PLS scatter plot of beads for 488.0 nm light (integrated matrix elements S11 + S12 in forward direction vs. S11−S12 in perpendicular direction). Inserted numbers indicate the diameter of the beads. Insert: part of curve for beads from 0 to 3 μm.

cies" in the measured integrated matrix elements are present in the calculated integrated matrix elements (Fig. 5B), but the existing amplitudes are not high enough to account for the observed patterns. This suggests that the beads cannot be considered as perfect round and homogeneous spheres. The production process of these beads entails the growth of polystyrene layers on a very small particle. This means that a non-isotropic distribution of the molecules could be present, for instance a radially symmetric distribution of the orientation or density of the molecules. This anisotropy of the beads may give rise to the observed differences from the theoretically predicted scatter plots. Further investigations on this subject are being made.

Light scattering signals can in principle be used to obtain a rapid spherical particle sizing method with extreme size-sensitivity. Figure 8A shows that the FLS signal is not monotonically dependend on the size, so for these high refractive spheres the FLS signals cannot be used as a direct measure of the size without taking into account the described behaviour. One can get a good idea of the size resolution from Figure 6A: one complete loop corresponds to about 0.13 μm size difference for a particle of about 7 μm. The size-sensitivity can even be enhanced by optimizing central detection angle, decreasing numerical aperture and wavelength. Additional sizing with for instance forward light scattering, could separate overlapping particles in the dot plots (see for instance Figure 7).

The Lissajous-like patterns are due to the high symmetry of the homogeneous spheres. Biological cells exhibit inhomogeneities and irregular forms, so in general we do not expect to measure Lissajous-like patterns with cells. However, it might be possible to see such effects in very homogeneous cell populations under certain conditions (very small numerical aperture, large cells, high relative refractive index).

The measurements reported here indicate that alignment of flow cytometers with beads of sizes in the micrometer range can give some problems. As is shown in Figure 2C the CV of perpendicular light scattering can be large although the CV of the size distribution is small. From Figure 8B it is clear that the CV of the measured perpendicular light scattering signals from beads with a very narrow size distribution will oscillate when increasing the average size. This effect is to a lesser extent also present for the FLS signals. In general our observations indicate that there is no linear relation between the CV of perpendicular light scattering and alignment quality when measuring calibration beads. Therefore, one should be very careful when the CV of perpendicular light scattering is used as an index of alignment quality.

CONCLUSIONS

In this article we have shown that Lissajous-like loops can occur in two-parameter scatter plots of calibration beads. We have shown that these effects are caused by extreme size-dependency of the perpendicular light scattering of spherical beads and can be described reasonably well with the Lorenz-Mie theory. These effects can be of importance for the interpretation of the measured CV of particles in the perpendicular direction.

LITERATURE CITED

1. Bakker Schut TC, Florians A, Van Der Werf KO, De Grooth BG: Flow cytometry signal processing and data acquisition with a personal computer using an RTI-800 multifunction A/D I/O Board. Rev Sci Instrum 64(11):3116–3120, 1993.
2. Barber PW, Hill SC: Light Scattering by Particles: Computational Methods. Advanced Series in Applied Physics, vol. 3. World Scientific Publishing Corporation, London, 1990.
3. Benson BC, McDougal DC, Coffey DS: The application of perpendicular and forward light scattering to asses nuclear and cellular morphology. Cytometry 5:515–522, 1984.
4. Bohren CF, Huffmann DR: Absorption and Scattering of Light by Small Particles. John Wiley & Sons, New York, 1983.
5. De Grooth BG, Terstappen LWMM, Puppels GJ, Greve J: Light-scattering polarization measurements as a new parameter in flow cytometry. Cytometry 8:539–544, 1987.
6. Gouesbet G, Grehan G, Maheu B: Localized interpretation to compute all the coefficients g(n,m) in the generalized Lorenz-Mie theory. J Opt Soc Am A 7:998–1007, 1990.
7. Gulari E: Latex particles size distribution from multiwavelength turbidity spectra. Part Charact 4:96–101, 1987.
8. Hoekstra AG, Doornbos RMP, Deurloo KEI, Noordmans HJ, De Grooth BG, Sloot PMA: Yet another face of Lorenz-Mie scattering: Mono disperse distributions of spheres produce Lissajous-like patterns. Appl Optics 33:494–500, 1994.
9. Lorenz LV: Upon the light reflected and refracted by a transparant sphere. Vidensk Selsk Shrifter 6:1–62, 1890.
10. McNeil PL, Kennedy AL, Waggoner AS, Taylor DL, Murphy RF: Light scattering changes during chemotactic stimulation of human neutrophils. Cytometry 6:7–12, 1985.
11. Mie G: Considerations on the optics of turbid media, especially colloidal metal sols. Ann Physik 25:377–442, 1908.
12. Mueller H: The foundation of optics. J Opt Soc Am 38:661, 1948.
13. Salzman GC, Singham SB, Johnston RG, Bohren CF: Light scattering and cytometry. In: Flow Cytometry and Sorting, 2nd ed., Melamed MR, Lindmo T, Mendelsohn ML (eds). Wiley-Liss Inc., New York, 1990, pp 81–107.
14. Sklar LA, Oades ZG, Finney DA: Neutrophil degranulation detected by right angle light scattering: Spectroscopic methods suitable for simultaneous analyses of degranulation or shape change, elastase release, and cell aggregation. J Immunol 133:1483–1487, 1984.
15. Sloot PMA, Figdor CG: Elastic light scattering form nucleated blood cells: Rapid numerical analysis. Appl Optics 25:3559, 1986.
16. Sloot PMA, Hoekstra AG, Van Der Liet H, Figdor CG: Scattering matrix elements of biological particles measured in a flow through system: Theory and practice. Appl Optics 28:1752–1762, 1989.
17. Terstappen LWMM, De Grooth BG, Visscher K, Van Kouterik FA, Greve J: Four-parameter white blood cell differential counting based on light scattering measurements. Cytometry 9:39–43, 1988.
18. Van De Hulst HC: Light Scattering by Small Particles, Dover Publications, Inc., New York, 1981.